Green's Functions, Noise, and Seismic Interferometry

Julien Chaput

May 15th 2008

Abstract

Recent developments in seismic imaging theory have verified a long-standing postulate concerning the recovery of earth's Green's function from seismic noise, the interest in this methodology being sparked by the annihilation of a need for source characteristics. Through the cross-correlation at two surface receivers of noise signatures originating at depth, one may retrieve the impulse response function between these two receivers, granted the noise source distribution is fairly continuous on a surface surrounding the medium of interest. In such a perfect scenario, only source contributions from stationary arrivals will interfere constructively in the spatial averaging, with all other spurious arrivals being canceled. Applications thus far are largely limited to surface wave Green's tensor recovery, as this simplifies the source distribution problem, though some efforts are underway to recover the full body wave Green's tensor in volcanic settings.

1. Introduction

Recent works by Wapenaar & Fokkema (2005), Snieder (2004), Campillo & Paul (2002), and a host of others have confirmed both theoretically and practically the 3D elastodynamic generalization of Claerbout's 1967 1D postulate, that is, that the autocorrelation of noise generated at depth at a surface station yields the reflection profile of the earth under that station. Naturally, using two different surface points instead of one yields the impulse response function between these points, as is indicated by the cartoon in figure 1.

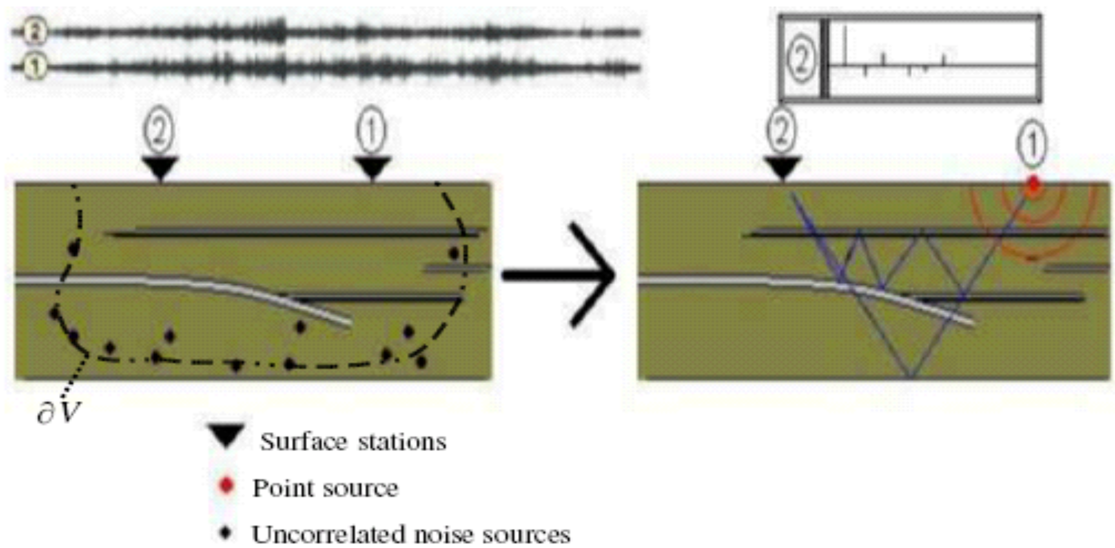

Figure 1: The cross-correlation of noise generated at depth at two surface stations yields the impulse response between these stations.

The draw of this methodology is that the source timing and particular source signatures become irrelevant, as they are annihilated in the cross-correlation. As such, in a highly scattering noisy environment, the aptly named seismic interferometry provides a potential inexpensive imaging technique where active source efforts and teleseismic geometries are impractical.

2. Theoretical considerations

For the sake of simplicity, the 1D acoustic case will be laid out, followed by the 3D acoustic generalization. The 3D elastodynamic case will simply be postulated, as its derivation is nearly identical to the acoustic case.

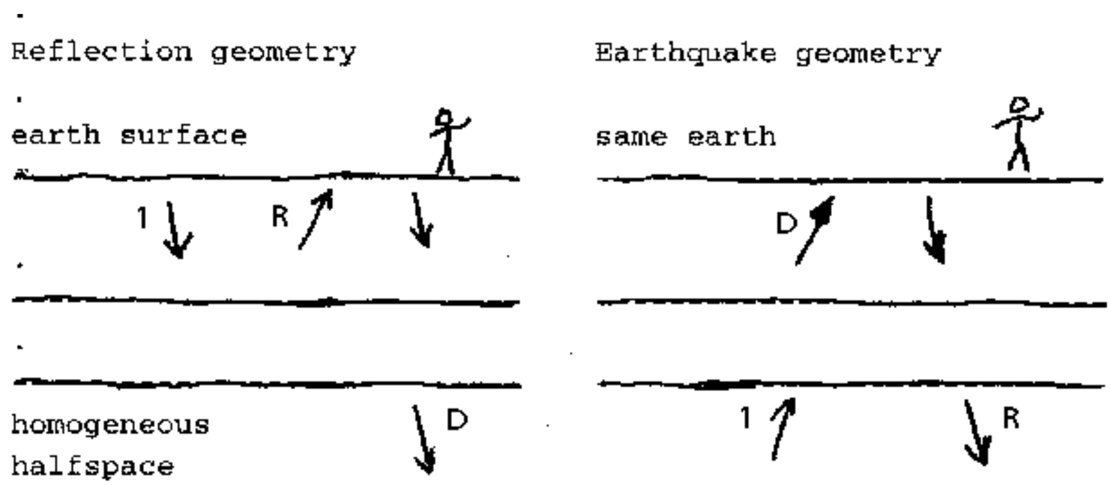

Figure 2: Cartoon demonstration of the 1D acoustic case (**Claerbout, J., personal site**)

Following Claerbout's 1967 postulate, we start with the reflection geometry setup described above, where D is the down going wavefield at any depth, and R the upcoming wavefield at any depth, as a consequence of a point source (delta function) fired at the surface (defined by "*1*"). Therefore, the down going wavefield anywhere in the medium can be expressed as:

$$D = 1 - R \tag{1}$$

The down going power flux in the frequency domain at any depth is therefore:

$$D^* D - R^* R = (1 - R^*)(1 - R) - RR^* = 1 - R - R^* \tag{2}$$

Where "*" indicates a complex conjugation. Beneath the layered medium (i.e. into the homogeneous medium), the down going energy flux is:

$$D^* D - R^* R = D_b^* D_b \tag{3}$$

where D_b is the down going wavefield in the homogeneous medium. As the down going energy flux must be conserved at all depths, this result is simply equal to the RHS of the previous equation. Thus:

$$R(\omega) + R^*(\omega) = 1 - D_b^*(\omega) D_b(\omega) \tag{4}$$

Taking the Fourier transform and applying source-receiver reciprocity for the "earthquake geometry":

$$R(t) + R(-t) = \delta(t) - D_s^*(-t)D_s(t) \tag{5}$$

where D_s is the upcoming wavefield at the surface in the earthquake geometry of Figure 2. Therefore, for this simple case, we have that the autocorrelation of the upcoming wavefield generated by an impulsive source at yields the vertical reflection profile of the layered medium.

The 3D acoustic case is slightly more complex, and we choose to follow the more deterministic derivation suggested by Wapenaar (2004). We start by considering the simplest case scenario (a 3D homogeneous fluid half space bound by a free surface) and state the equation of motion:

$$j\omega\rho v_i + \partial_i p = f_i \tag{6}$$

and the stress-strain relation:

$$j\omega\kappa p + \partial_i v_i = q \tag{7}$$

where j is the imaginary unit, f_i the external body force term (which will be set to zero), and q a source term with units of volumetric rate injection density. We then consider the so-called De Hoop's *interaction quantity* as defined by,

$$\partial_i\left(p_A v_{i,B} - v_{i,A} p_B\right) \tag{8}$$

which relates the pressure and particle velocity fields of two given states (e.g. two receivers) in a medium. Substituting (6) and (7) into (8), integrating over a volume V which encompasses the medium of interest and applying Gauss' theorem, we obtain:

$$\int_V \left(p_A^* q_B - v_{i,A}^* f_{i,A} - q_A^* p_B + f_{i,A}^* v_{i,B}\right) d^3x = \oint_{\partial V} \left(p_A^* v_{i,B} - v_{i,A}^* p_B\right) n_i d^2x \tag{9}$$

which is called the reciprocity theorem of the correlation type. Here, we choose an impulse source term and null external body forces, so that:

$$\begin{aligned} q_{A,B}(x,\omega) &= \delta\left(x - x_{A,B}\right) \\ p_{A,B}(x,\omega) &= G\left(x, x_{A,B}, \omega\right) \\ v_{i,A,B}(x,\omega) &= -\left(j\omega\rho(x)\right)^{-1} \partial_i G\left(x, x_{A,B}, \omega\right) \end{aligned} \tag{10}$$

where we define $G\left(x, x_{A,B}, \omega\right)$ as the frequency domain Green's function at a point *x*, from a source at a point x_A. Substituting (10) in (9), we obtain:

$$2\Re\left[G(x_A,x_B,\omega)\right] = \oint_{\partial V} \frac{-1}{j\omega\rho(x)} [G^*(x_A,x,\omega)\partial_i G(x_B,x,\omega) - \left(\partial_i G^*(x_A,x,\omega)\right)G(x_B,x,\omega)] n_i d^2x \tag{11}$$

which is, though theoretically accurate, difficult to implement, as it requires dipole and monopole source responses as well as the ability to record every source response over ∂V individually. Several practical approximations must therefore be made. First off, a high frequency approximation is assumed, so as to express the dipole response in terms of a monopole response:

$$\partial_i G(x_A,x,\omega)n_i \approx -j\frac{\omega}{c(x)}G(x_A,x,\omega) \tag{12}$$

Next, we must assume that the integration surface defined by ∂V is fairly irregular, so as to cancel out contributions from reflectors outside the medium of interest. Finally, to circumvent the integral, we suppose that our sources are uncorrelated white noise sources, so that:

$$p^{obs}(x_{A,B},\omega) = \oint_{\partial V} G(x_{A,B},x,\omega)N(x,\omega)d^2x \tag{13}$$

where $N(x,\omega)$ is a noise source which obeys:

$$\left\langle N^*(x,\omega)N(x',\omega)\right\rangle = \delta(x-x')S(\omega) \tag{14}$$

Here, all the source responses can be read simultaneously, as the integral has been replaced by a spatial (or temporal) average (e.g., a correlation stack) defined by the angular brackets. Using these assumptions along with (11) yields:

$$2\Re\left(G(x_A,x_B,\omega)\right)S(\omega) \approx \frac{2}{\rho c}\left\langle p^{obs*}(x_A,\omega)p^{obs}(x_B,\omega)\right\rangle \tag{15}$$

This equation is well suited for practice, as it states that the impulse response between two surface receivers *A* and *B* can be obtained by the cross-correlation of uncorrelated noise sources generated at depth, granted the existence of a complete source distribution around the medium of interest (i.e. no significant source gaps on ∂V). The 3D elastodynamic version of this equation is derived similarly, and yields:

$$\begin{aligned} 2\Re\left[G^{v,f}_{p,q}(x_A,x_B,\omega)\right] &= \frac{2}{j\omega\rho}\int_{\partial V}\left[\partial_i G^{v,\phi}_{p,K}(x_A,x_B,\omega)\right]^* G^{v,\phi}_{q,K}(x_B,x_A,\omega)n_i d^2x \\ &\approx \frac{2}{\rho c_p}\left\langle v^{obs*}_p(x_A,\omega)v^{obs}_q(x_B,\omega)\right\rangle \end{aligned} \tag{16}$$

where, for $G^{v,f}_{p,q}(x_A,x_B,\omega)$, *v* and *f* define the observed and source quantities (i.e. velocity Green's function, force source term), and *p* and *q* define the components of the observed wavefield and the component of the source.

As a final, but critically important theoretical point, it must be noted that only sources located within one Fresnel zone of a stationary point will stack constructively after the spatial averaging. Mathematically speaking, this means that the main contributions to the true Green's function come from the slowest varying points of the integrand in (16). The following figure considers a very simple case, in which there is a very limited distribution of sources to one side of a station pair sitting over a homogeneous half-space with a single embedded reflector of limited length.

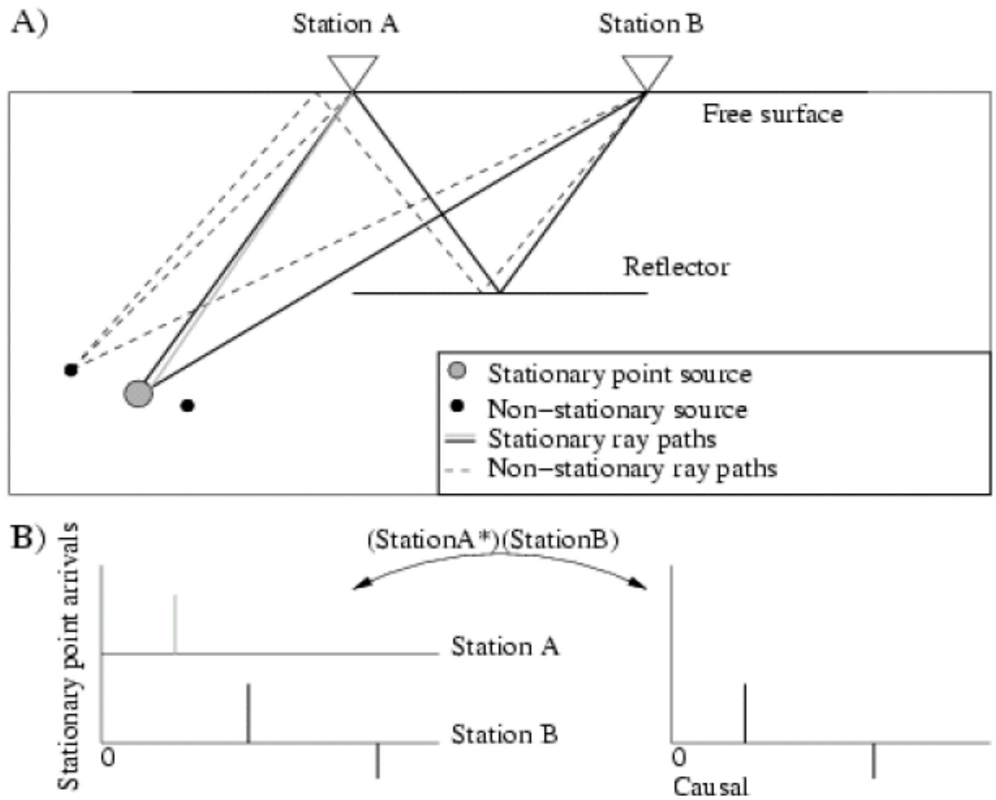

Figure 3: Simple case scenario. The direct and reflected paths are correlated at both receivers, though only the lag yielded for the reflected path is correct, as the stationary point for the direct inter station surface wave is a surface source. Note also that the non-stationary sources will provide non-physical ray paths, and their contributions are generally eliminated in the stack.

We can draw from this figure that there exists a unique set of stationary points (for both symmetric sides of the Green's function) for each reflector in the subsurface. When the medium becomes complex, a more complete source distribution is required to recover all true contributions to the Green's function. Figure 4 shows another example of the stationary point phenomena.

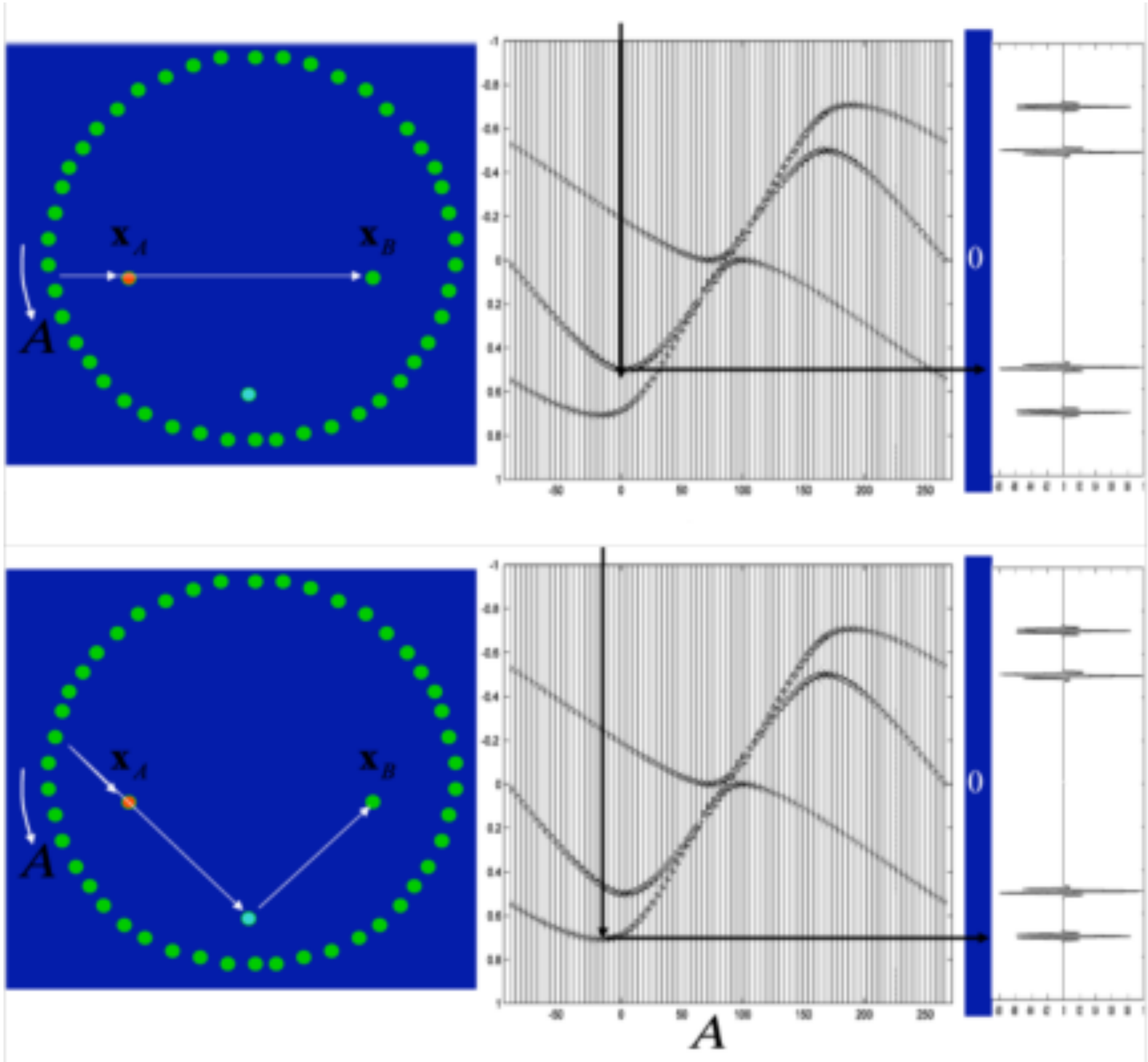

Figure 4: Second simple scenario, featuring two receivers, X_A and X_B and one scatterer (light blue dot) embedded in a homogeneous medium surrounded by sources (green dots), for the direct and singly scattered paths. As the source location changes along *A*, the causal and acausal cross-correlation curves (center panel) vary quickly until they hit the stationary point arrival, which stacks constructively in the resulting Green's function (far right). Note the symmetry of causal and acausal portions, and the lack of any spurious arrivals once the stack is taken. (**Wapenaar, K., SEG 2005)**

Therefore, to apply this theory successfully, it is important to remember that for an ideal case, true contributions to the Green's function are the result of constructive interference from stationary point sources at depth, though when lacking large datasets, spurious arrivals may give rise to faulty interpretations.

3. <u>The surface wave problem</u>

Though there is still some debate as to the importance of the particular characteristics of the noise wavefield (e.g. a necessity for modal equipartioning), there has nonetheless been a substantial amount of applications recently, mostly concerning surface wave ambient noise tomography, with only a few pertaining to the recovery of the body wave Green's tensor (Roux et al, 2005, Chaput & Bostock, 2007). As the surface wave case only deals with the direct arrival defined by figure 4, and as there exists an abundance of natural surface wave sources (ambient noise, Rayleigh waves from seismic coda), it is much more robust and easier to apply than the body wave case. Campillo & Paul were the first to apply surface wave Green's tensor recovery in 2002, as is evidenced by figure 5.

Recent efforts by Brenguier et al (2006) have taken this experiment one step further, by performing a tomographic inversion based on dispersion curves of Rayleigh waves obtained at the Piton de la Fouraise Volcano (figure 6). They managed to perform a limited depth inversion as well, providing a rough image of a dipping magma chamber, demonstrating the usefulness of this method in highly scattering volcanic settings.

Similar efforts are currently underway at the Mount Erebus volcano, Antarctica, in an attempt to extract a rough velocity model based on ambient noise tomography (Figure 7). The recently expanded seismic network on Mt Erebus in 2007-2008 will provide adequate station spacing for Rayleigh wave recovery. There are also early attempts at a body wave Green's function recovery using Strombolian eruption coda, as deep reflectors have been observed in an earlier analysis of the wavefield (Henderson, 2007).

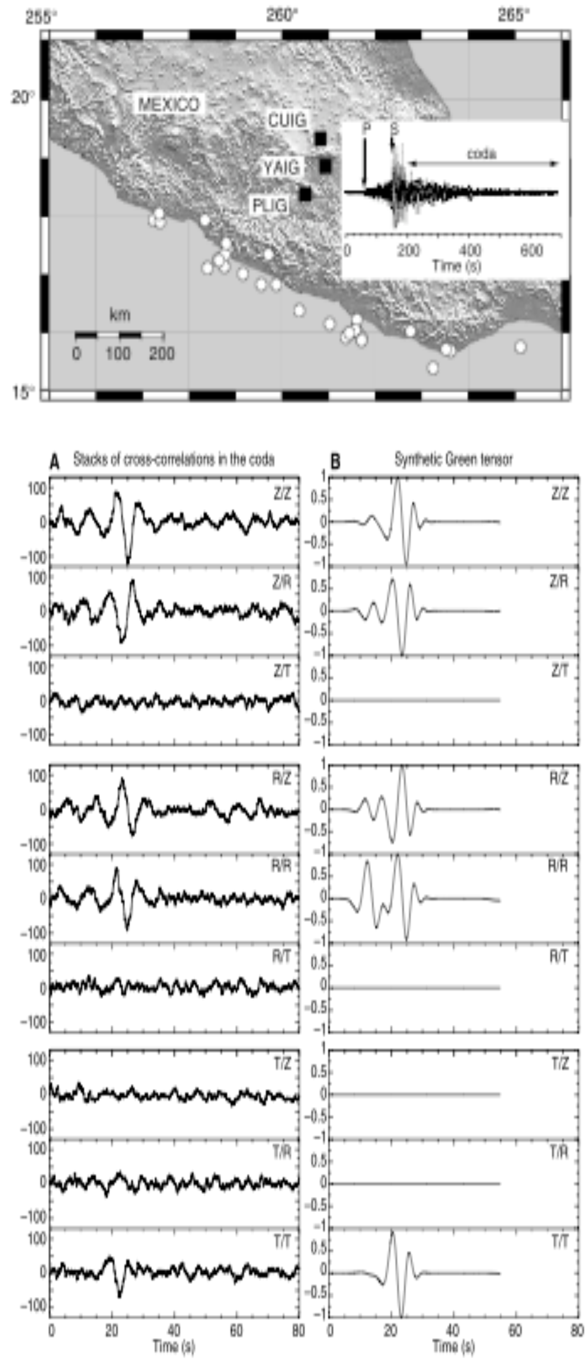

Figure 5: Results from Campillo & Paul (2002). Cross-correlations of 18 months of seismic coda clearly yield the surface wave Green's tensor, theoretically defined by the synthetic on the right.

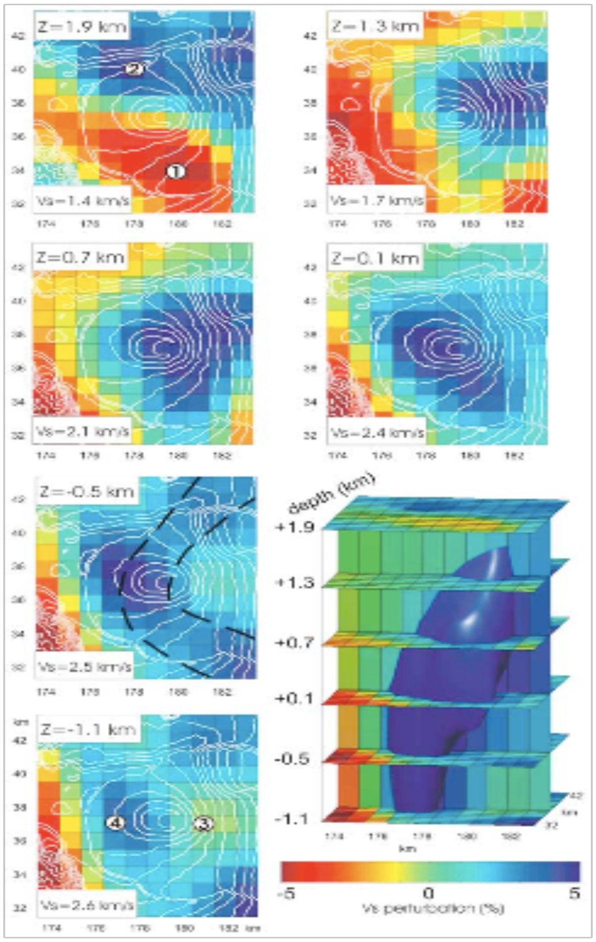

Figure 6: Results from Brenguier et al 2007, showing a tomographic image (left panel) recovered from Rayleigh wave group velocity estimates (below) at the Piton de la Fournaise volcano. Note the presence of a high velocity anomaly, interpreted as the magma column/chamber.

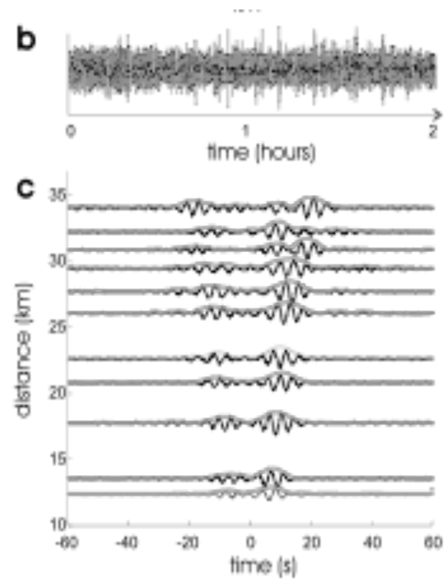

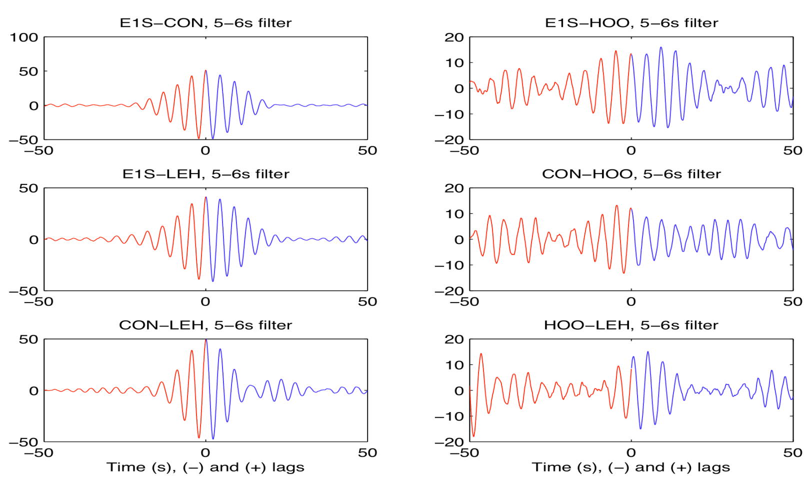

Figure 7: Narrow band Rayleigh wave recovery at Mt Erebus volcano, Antarctica. Larger station spacing will help pick group velocity arrivals to construct dispersion curves.

4. The body wave problem

Currently, a full body wave Green's tensor recovery using seismic interferometry has not successfully been accomplished, though synthetics have shown that it is very much a possibility given the right scenario. The difficulty, as stated in the theory, resides in the necessity of having a full source distribution around the medium of interest, which, for natural sources, is very difficult. Figure 8 displays one such synthetic, developed for a marine seismology case.

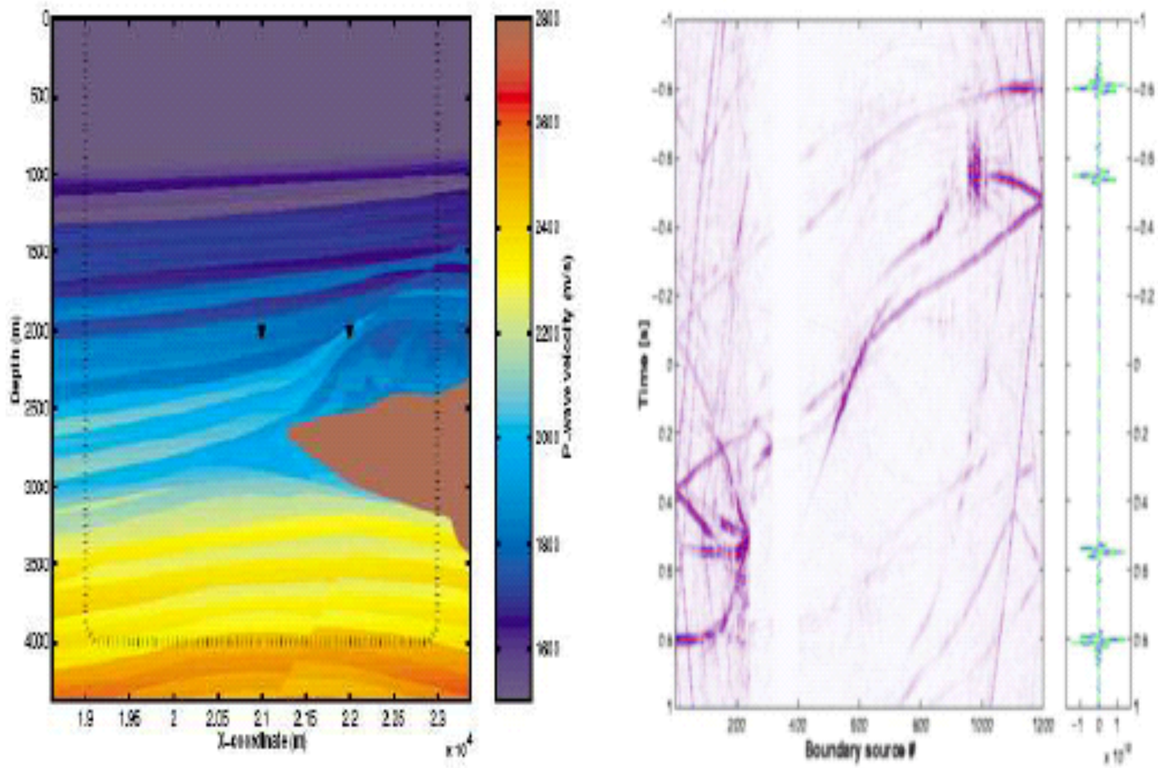

Figure 8: Synthetic from Van Manen et al, 2005, featuring two receivers (black triangles) embedded in a medium with a single large reflecting feature (brown shape) surrounded by sources (dotted line). As in figure 4, each source is fired, and the response is cross-correlated at the receivers, generating the figure in the right panel. Once stacked, the direct and reflected arrivals are recovered.

Notice how, as soon as the medium acquires some complexity, the right panel becomes rather complicated, with sections of strong spurious arrivals occuring everywhere. If the source distribution is not in fact continuous, it is fairly easy to imagine some of these arrivals finding their way into the stack. This problem might however be solved in cases where one has access to a large temporal span of data containing a fair amount of source variability.

5. Conclusions and potential works

Seismic interferometry has been shown to be effective in scattering media for surface wave recovery and tomography, though examples of applicability to body wave tomography are lacking. The main issue when dealing with a body wave scenario is that non-anthropogenic sources will not tend to be distributed evenly over a surface encompassing a medium of interest. As a result, the recovered Green's function, though containing some true path information, may be difficult to decipher, as it is easy to see by stacking only a portion of the arrivals in figure 8. Nonetheless, there are currently efforts to use the coda of Strombolian eruptions on Mt Erebus to this end, as it is hypothesized that the volcano's extremely scattering medium might cause the scattered wavefield to arrive from all stationary points under a given receiver pair of the newly expanded seismic array, while still containing relatively high frequencies. Thus far, same station autocorrelations have indeed yielded very late coherent scattered arrivals.

6. References

Brenguier, F.N. (et al), **3-D surface wave tomography of the Piton de la Fournaise volcano using seismic noise correlations**, Geophysical Research Letters, Vol.34, 2007

Campillo, M., Paul, A., **Long-range correlations in the diffuse seismic coda**, Science, Vol.299, 2003

Chaput, J., Bostock, M.G., **Seismic interferometry using non-volcanic tremor in Cascadia**, Geophysical Research Letters, Vol. 34, L07304, 2007

Henderson, B., **Analysis of seismic similarity in Strombolian eruptions for Mount Erebus, Antarctica**, Master thesis, 2007

Roux, P. (et al), **P-waves from cross-correlation of seismic noise, Geophysical Research Letters**, Vol.32, L19303, 2005

Snieder, R., **Extracting the Green's function from the correlation of coda waves: a derivation based on stationary phase**, Phys.Rev.E, Vol 69, Issue 4, 2004

Van Manen, D.J., Robertsson, J., **Modeling of wave propagation in inhomogeneous media**, Phys. Rev. Lett., Vol. 94, 2005

Wapenaar, K., Fokkema, J., **Green's function representations for seismic interferometry**, Geophysics, special issue on seismic interferometry, 2005